

Spectral Measurements and Visualization of the Plasma Processes during Effective Heating in Lower Hybrid Experiment on FT-2 Tokamak

S.I. Lashkul, A.B. Altukhov, A.O. Bogdanenko*, V.V. Dyachenko, L.A. Esipov, M.Yu. Kantor, D.V. Kouprienko, A.D. Lebedev, A.P. Sharpeonok

A.F.Ioffe Physico-Technical Institute, Politekhnikeskaya 26, 194021, St.Petersburg, Russia,

*St.Petersburg State Polytechnical University, St.Petersburg, Russia

In recent experiments at FT-2 tokamak the main attention was paid to the study of the plasma periphery region ($\Delta r = 4\div 6\text{cm}$), where the Internal Transport Barrier (ITB) during additional Lower Hybrid Heating (LHH) is formed. LHH experiment demonstrates the L-H transition with hydrogen recycling decrease and density turbulence suppression at the plasma periphery and SOL after RF pulse end [1]. The paper presents both the spectral measurements needed for plasma radial electric field calculation and the first experience using the TV set as receiver of the monochromatic radiation.

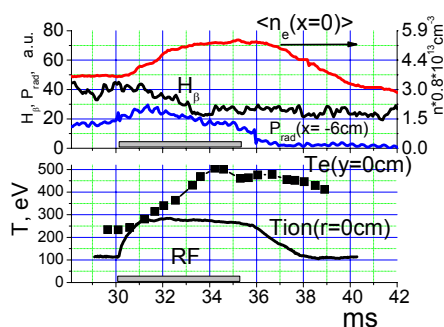


Fig. 1

Here $\langle n_e(x=0\text{cm}) \rangle$ is central average density, $T_e(y=0\text{cm})$ $T_i(r=0\text{cm})$ are central electron and ion temperatures. H_β - spectral line intense. Decrease radiation losses P_{rad} shown for high field side chord $X = -6\text{cm}$.

the middle of a $\Delta t_{pl} = 60\text{ms}$ plasma shot. Fig. 1 (#061505 experimental run [2]) depicts the plasma parameters and their changes during LHH. Chord profiles of the line of sight averaged density $\langle n_e \rangle$ are measured by 2mm interferometer, the electron temperature $T_e(y)$ is measured by the laser Thomson scattering (TS) diagnostics, where y is the coordinate of the vertical laser beam probe. The ion temperature $T_i(r)$ is measured by Nuclear Particle Analyzer (NPA) and spectroscopic diagnostics. The plasma central parameters rise when

Table 1

$T_i^{LHH}(r=0\text{cm})/T_i^{OH}$	$T_e^{LHH}(r=0\text{cm})/T_e^{OH}$	$\Delta T_e^{LHH}(r=0\text{cm})/T_e^{OH}$	$P_{rad}^{LHH}/P_{rad}^{OH}$	$N_e^{LHH}(r=0\text{cm})/N_e^{OH}$
2.6	1.8	0.78	2.1	1.5

additional heating power $P_{LHH} = 160\text{kW} \approx 2P_{OH}$ is applied (see Table 1). The radiation losses rise during additional heating is also recorded. These table data and their profiles (see

profiles versus to the magnetic surfaces radii in [3]) demonstrate the efficiency of the LH heating [3]. It is remarkable, that the central electron temperature increases as well as T_i and, moreover, it remains at higher level for about 5ms after RF pulse switch off. Drop down of the $H_\beta(481.8\text{nm})$ spectral line intensity (at 34ms), as well as fast radiation losses decrease for edge bolometer chord at high field side, $x = -6\text{cm}$, indicates an L - H transition. The L-H transition results in the rise of the energy confinement time in the post heating phase in comparison with the initial OH phase (by about two times — from $\tau_{OH}=0.8\text{ms}$ to $\tau_{PostLHH}=2\text{ms}$). The additional experimental data are needed to specify the physical processes,

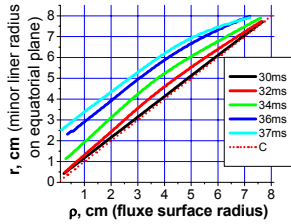


Fig. 2
The shifts of the circular flux surface (FS) lengthwise of the R

in particular, the periphery ion temperature and the poloidal plasma rotation, which are required for radial electric field E_r calculation. The rise of radial electric field shear could be responsible for transport barriers formation observed at LHH [2]. That problem is realized by spectral measurements of Doppler broadening and the Doppler shift of the impurity line profiles [4]. Such measurements are rather difficult because during additional heating a small shift (without any plasma current disruptions) of the plasma column along the major radius R is observed, which doubles the difficulties of the interpretation of spectroscopic measurements. The Fig. 2 depicts the summary shifts (plasma core and Shafranov's shifts) of the circular flux surface (FS) along the major radius R during LHH experiment (#053106 run [5]). Those FS shifts (calculated for different shot moments by inversion processing of the density chord profiles) have to be taken into account when radial profiles of the plasma parameters are calculated. The Fig. 3 presents the consequence of inverse spectral data processing for CIII(464.7nm) [$2s3s(^3S_1) - 2s3p(^3P_2)$] local emissivity profiles, when FS shift is taken account.

Spectral measurements

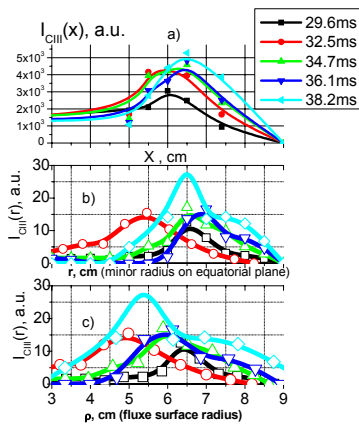


Fig. 3
a) Part of $I_{CIII}(x)$ chord profiles; b) $I_{CIII}(r)$ local emissivity vs minor liner radius on equatorial plane; c) $I_{CIII}(\rho)$ local emissivity vs FS radii

I. Spectral measurements in the visible region spectra are made by two monochromators providing observation of fast parameters changes at the periphery of the plasma core [4]. Spectral resolution of the monochromator M1 (f/7, grating 1200 g/mm) in the second and third orders is 0.5nm/mm and 0.27nm/mm, respectively, which is enough to determine the variables $\Delta T_i \leq 5\text{ eV}$ and $\Delta v_\theta \leq 0.5\text{ km s}^{-1}$ at $\Delta t \sim 1\text{ms}$ time smoothing. Instrumental parameters in the second and third orders are $\Delta\lambda_{inst} = 0.036\text{nm}$ and 0.022nm, respectively. The optical trace of the M1 consists of 90mm, f/9 quartz lens, providing the spatial resolution of 6 mm at the middle horizontal plane of the vacuum chamber. Spectral line emissivity profile measurements by monochromator M1 are realized shot by shot using a series of the identical tokamak discharges. Monitoring of the

line-chord-integrated intensity during such spectral measurements is provided by the second monochromator M2 (f/2.5, 1200g/mm, 2nm/mm) against vertical diameter. The measured spectral line emissivity $I(\lambda)_l$ profile involve the Doppler broadening, Doppler shift of impurity spectral lines taking into account the line-of-sight integral effect (and instrumental function) arising from the experimental arrangements. The line-of-sight integrated spectral profile $I(\lambda)_l$ for chord “ $x = l$ ” is Gaussian with localized widths, shifts and heights presented in forms:

$$I(\lambda)_l \sim \int_l I_0(x) \exp\left[-\frac{2.77(\lambda - \lambda_v(x))^2}{\lambda_T^2(x)}\right] dx \sim \int_{r_0}^a \frac{I_0(r)}{\lambda_T(r)} \frac{r}{\sqrt{r^2 - r_0^2}} \exp\left[-\frac{2.77(\lambda - \lambda_v(r))^2}{\lambda_T^2(r)}\right] dr \quad (1)$$

Here the second integral is written in cylindrical coordinates when $x^2 = r^2 - r_0^2$, where r_0 is the line-of-sight distance. Doppler broadening is $\Delta\lambda_D = \lambda_T = 7.7 \times 10^{-5} (T_i / \mu)^{1/2} \lambda_0$ and Doppler shift is $\Delta\lambda = \lambda_v = \lambda_0 (V_\theta / c) \cos\beta$, where V_θ is poloidal ion velocity, β is the angle between the line of sight and flux surface, $\cos\beta = r_0/r$. For the deconvolution of the chord measurements in order to take into account the line integration effects we used handle modelling using $\lambda_v(r)$ and λ_T as free fitting parameters in expression (1). The results of such iteration method are presented for (#053106, [5]) experimental run (see Fig. 4). Fig. 4a

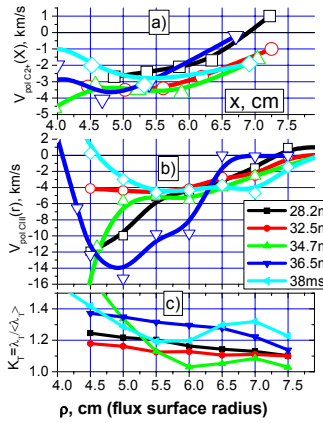


Fig. 4

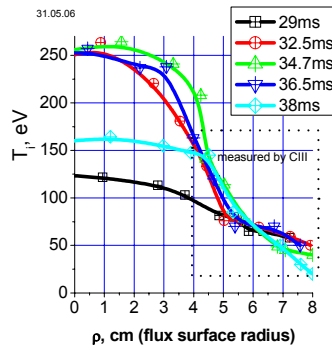


Fig.5

depicts the experimental C^{2+} poloidal velocity $V_{\theta,C^{2+}}(r)$ with the line-of-sight integral effect versus chord location corrected on the plasma core shift. Fig 4b depicts the $V_{\theta,C^{2+}}(r)$ after the deconvolution of the chord measurements by iteration method mentioned above. Fig. 4c presents the line Doppler broadening correction factor

$$k_T = \lambda_T(\text{fitting parameter})(\rho) / \langle \lambda_T \rangle_{(\text{experiment})}$$

The ion temperature profiles $T_i(r)$ measured by NPA and spectral diagnostics with an account of the k_T are presented in Fig. 5. The data calculated by Doppler broadening are marked by the dotted box and demonstrate the good agreement with NPA data in region $\Delta r = 4 \div 5$ cm where both diagnostics overlap, and where ITB is formed. The radial electric field E_r is derived from the poloidal rotation velocity and pressure gradient of C^{2+} impurity measured with spectroscopy [4] using the radial force balance equation [see Ref [6] for example]. Those data are presented and discussed in another paper of that conference [5].

II. The neutral hydrogen recycling decrease during LHH and L-H transition was one of the subjects of the investigation by spectroscopic diagnostics. For those measurements the black and white upgraded television video camera VC (VNC-542) has been used as light receiver of the M2 monochromator. The maximal sensitivity of the VC is within spectral range 450nm – 750nm [3]. Spectral resolution is 2A/pix. The cord profiles along vertical diameter observed in the hydrogen lines are detected with the space resolution 20pix/cm.

The application of the video system with appropriate software has enabled us to obtain the time sequence of line of sight integrated intensity profile $I(\lambda)_l$ at 2.5 ms time intervals and 1ms exposure time. A number of the H_α (656,3nm) line integral radiation intensity profiles against vertical diameter are obtained during one shot as well as H_β (468nm) profiles. The fast decrease of the chord intensity profiles of H_α and H_β spectral lines after 34 ms [3] have been observed (see Fig. 1 also). That fact could be understood as decrease of the hydrogen recycling near a plasma periphery and following to the idea of the authors of the [7, 8] could be explained by the atom/molecular ratio change. The population distribution over the excited atomic levels depends on whether these atoms are produced from CX atomic hydrogen or they are produced from molecular hydrogen desorbed from the cold wall. The method to determine the atomic hydrogen and molecular hydrogen density is

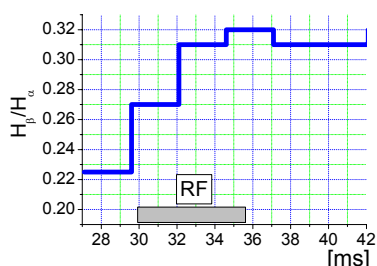


Fig. 6

based on the value of the ratio of observed Balmer line intensities of atomic hydrogen. For the plasma density $n_e \sim (0.5 \div 1.0)10^{13} \text{cm}^{-3}$ corresponding to the plasma periphery, the ratio between radiation in spectral lines of hydrogen H_α and H_β can be changed from a value of ~ 1.5 (for plasma with 100% molecular hydrogen) up to value of ~ 3 (for plasma with 100% atoms hydrogen content) [7]. The LHH experiment shows that the intensity ratio of hydrogen emission lines H_β/H_α at the periphery changes from $0.2 \div 0.22$ to $0.30 \div 0.32$ during LHH and L - H transition (see Fig. 6). Altogether this trend indicates at arbitrary decrease of hydrogen molecular content, that seems to be a result of reducing of the direct interaction of the plasma core with the limiter and chamber wall which is origin of cold molecular fluxes. The bolometric radiation losses data presented in Fig. 1 also indicate the effect of decrease of the plasma – wall radiation load observed during L-H-mode transition. Recent experimental run (#032907) with direct plasma core observation by VC (without of the M2) through vertical port permits to visualize the effect of the shift ($\Delta R \sim 1.5 \text{cm}$) outward plasma core, small decrease of its diameter ($\Delta r \sim 1 \text{cm}$) during LHH with sharp decrease periphery radiation detected within 450nm – 750nm spectral range.

This work supported by RFFR 05-02-17761, 07-02-00895 and RF Schools NSH-5149.2006.2 grants.

References

1. S.I. Lashkul, et al. Czechoslovak Journal of Physics (2002) 52 (10) 1149-1159
2. V Rozhansky. Plasma Phys. Control. Fusion 46 (2004) A1–A17
3. Lashkul S.I. et al. Proc. 21st IAEA Conf. on Fus. Energy (Chegdu 2006) IAEA/EX/P6-18
4. S.I. Lashkul, V.N. Budnikov, V.V. Dyachenko et. al. Pl. Phys. Cont. Fusion 44 (2002) 653
5. S.I. Lashkul et al. Proc. of the 34th EPS and Pl. Phys. Warshava, 2007, P2.055
6. Field A.R., Fussmann G., Hormann J.V. Nucl. Fusion 32 (1992) 1192
7. Keiji Sawada, Kouji Eriguchi and Takashi Fojimoto. J. Appl.Phys.73(12), 15 June 1993
- 8 U. Fantz et al. 26th EPS Conf., ECA Vol 23J(1999) 1549-1552